Unusually severe muscular dystrophy upon in-frame deletion of the dystrophin rod domain and lack of compensation by membrane-localized utrophin

Svetlana Gorokhova, Joachim Schessl, Yaqun Zou, Michele L. Yang, Peter T. Heydemann, Robert L. Sufit, Katherine Meilleur, Sandra Donkervoort, Livija Medne, Richard S. Finkel, et al.

Unusually severe muscular dystrophy upon in-frame deletion of the dystrophin rod domain and lack of compensation by membrane-localized utrophin

Svetlana Gorokhova, M.D., Ph.D.[1,2,3]*, Joachim Schessl, M.D.[4,5]*, Yaqun Zou, M.D.[1]*, Michele L. Yang, M.D.[4,6]*, Peter T. Heydemann, M.D.[7], Robert L. Sufit, M.D.[8], Katherine Meilleur, Ph.D.[9], Sandra Donkervoort, M.S.[1], Livija Medne, M.S.[4], Richard S. Finkel, M.D.[4,10], Carsten G. Bönnemann, M.D., habil.[1, §]

[1] National Institute of Neurological Disorders and Stroke, National Institutes of Health, Bethesda, MD, 20892, USA

[2] Aix Marseille Univ, INSERM, MMG, U 1251, Marseille, 13005, France.

[3] Department of Medical Genetics, Timone Children's Hospital, AP-HM, Marseille, 13005, France.

[4] The Children's Hospital of Philadelphia, Pennsylvania Muscle Institute, Division of Neurology, University of Pennsylvania School of Medicine, Philadelphia, PA, 19104, USA [5]

Friedrich-Baur-Institute, Department of Neurology, Ludwig-Maximilians University of Munich, 80336, Germany

[6] Children's Hospital Colorado, Department of Pediatrics and Neurology, Aurora, CO, 80045, USA

[7] Department of Pediatrics and Neurology, Rush University Medical Center, Chicago, IL, 60612, USA

[8] Davee Department of Neurology, Northwestern University Feinberg School of Medicine, Chicago, IL, 6061, USA

[9] Research and Clinical Development, Neuromuscular Development Unit, Biogen, 300, Binney Street, Cambridge, MA, 02142, USA

[10] Center for Experimental Neurotherapeutics, St Jude Children's Research Hospital, Memphis, Tennessee, 38105, USA

* Drs. S. Gorokhova, J. Schessl, Y. Zou and M.L. Yang contributed equally to this article.

§ Lead contact

Lead contact:

Carsten G. Bönnemann, M.D.

carsten.bonnemann@nih.gov

Summary

Background

Utrophin, a dystrophin homologue, is consistently upregulated in muscles of patients with Duchenne muscular dystrophy (DMD) and is believed to partially compensate for the lack of dystrophin in dystrophic muscle. Even though several animal studies support the idea that utrophin can modulate DMD disease severity, human clinical data is scarce.

Methods

We describe a patient with the largest reported in-frame deletion in the *DMD* gene, including exons 10 to 60 and thus encompassing the entire rod domain.

Findings

The patient presented with an unusually early and severe progressive weakness, initially suggesting congenital muscular dystrophy. Immunostaining of his muscle biopsy showed the mutant protein was able to localize at the sarcolemma and stabilize the dystrophin-associated complex. Strikingly, utrophin protein was absent from the sarcolemmal membrane despite the upregulation of utrophin mRNA.

Conclusions

Our results suggest that the internally deleted and dysfunctional dystrophin lacking the entire rod domain may exert a dominant negative effect by preventing upregulated utrophin protein from reaching the sarcolemmal membrane and thus blocking its partial rescue of muscle function. This unique case may set a lower size limit for similar constructs in potential gene therapy approaches.

Funding

This work was supported by a grant from MDA USA (MDA3896) and by grant number R01AR051999 from NIAMS/NIH to C.G.B.

Keywords

Dystrophin, utrophin, DMD, Duchenne muscular dystrophy, congenital, deletion

Introduction

Dystrophin deficiency is associated with Duchenne muscular dystrophy (DMD) caused by out-of frame deletions in the *DMD* gene in 60-65% of cases, while in-frame deletions are usually associated with the milder Becker muscular dystrophy[1,2]. Several animal studies suggested that sarcolemmal upregulation of utrophin, an autosomal homologue of dystrophin, can functionally replace dystrophin in dystrophin-deficient muscle fibers[3–5]. However, only a few human studies point to its functional compensatory role in disease [6–9]. We describe an unusually severely affected patient with a large in-frame dystrophin deletion of the entire rod domain, which appears to exert an additional dominant negative effect on compensatory utrophin localization at the plasma membrane, supporting the notion that utrophin upregulation normally ameliorates the dystrophin-deficient phenotype.

Results

CASE REPORT

The family history was unremarkable with no history of myopathy, cardiomyopathy, or consanguinity. Early hypotonia was noted and at six months of age, motor milestones were already delayed, he sat unassisted at 12 months, stood unassisted at 15 months when placed in standing, and ambulated by 18 months of age with a waddling gait and frequent falls after being placed in standing position. Examination at three years and nine months of age revealed a waddling gait on the forefoot, marked proximal muscle weakness in the arms and legs, bilateral Achilles tendon and finger flexor contractures, calf hypertrophy, and significant lordosis (Figure 1A, Suppl. video). He still could not arise from the floor or roll from a supine position and had head lag on traction. Serum creatine kinase levels were highly elevated to 57.103 IU/L (normal: 75-230 IU/L). A muscle biopsy at three years of age revealed dystrophic changes with marked fiber size variation, internalized nuclei, necrosis and increased endomysial and perimysial connective tissue. On examination at seven years of age, he was non-ambulatory and profoundly weak. Proximal weakness was greater than distal, with loss of antigravity strength in all proximal muscles. However, with elbow support he was able to eat with his fingers, support his head in a seated position, and sit with precarious balance. He had mild facial weakness with transverse smile. Deep tendon reflexes were decreased throughout. There were significant but symmetrical hip contractures and significant contractures of the Achilles tendons and knees. He also had contractures of the long finger flexors and wrists, resulting in ulnar deviation. His spine was still flexible with scoliotic and kyphotic posture while sitting. ECG and echocardiogram were both normal. At age nine years and seven months, he suffered from an intermittent respiratory illness and died due to cardiac arrest in the setting of an airway plug.

PCR amplification of patient's genomic DNA revealed a deletion within the *DMD* gene encompassing exons 10 to 60 (Figure 1B). RT-PCR analysis of muscle RNA using primers placed in exons 9 and 62 allowed amplification and sequencing of the resulting new junction between exons 9 and 61, confirming that the patient's intragenic deletion preserved the reading frame of the *DMD* mRNA (Figure 1C). Deletion of the exons 10 to 60 is predicted to produce an internally deleted dystrophin protein lacking almost the entire central rod domain, where the end of the hinge 1 is joined directly to the final 12 amino acids of repeat 24 (Figure 1E), as well as remove isoforms Dp260, Dp140 and Dp116. The presence of this predicted dystrophin-derived protein was confirmed by western blot of patient's muscle tissue using two anti-dystrophin antibodies – one directed against the central rod domain and the other one specific to the C-terminal of dystrophin (Figure 1D). Consistent with the western blot results, immunohistochemical analysis of the patient's muscle biopsy using the central rod domain specific antibody (DYS1) and the N-terminal part specific antibody (DYS3) showed no staining (Supplemental Figures 1A and D), since the deletion is expected to remove the DYS1 and DYS3 epitopes (Figure 1E). Staining with the C-terminal specific antibody (DYS2) however revealed strong cell membrane-based signal in most myofibers (Supplemental Figure 1G). Muscle tissue from patient with the *DMD* del ex10-60 showed relatively normal expression of β-dystroglycan (Supplemental Figures 1J-L) and γ-sarcoglycan (Supplemental Figures 2J-L), suggesting integrity of the dystroglycan complex and the associated glycoprotein complex.

The appearance of strong C-terminal dystrophin sarcolemmal staining contrasted with the severe clinical presentation of the patient. To explore this intriguing observation, we investigated the expression and localization of utrophin, the highly homologous dystrophin-related protein that is consistently upregulated in DMD patients and is thought to partially compensate for the absence of dystrophin. Western blot analysis revealed an increase of utrophin protein in muscle lysates from both our patient and a typical DMD patient (Figure 2A). However, in striking contrast to the expected cell membrane utrophin labelling observed in DMD patients (Figure 2D, Supplemental Figures 2D-F), utrophin staining was intracellular in most muscle cells in the patient with the ex10-60 deletion and absent at the sarcolemma (Figure 2C, Supplemental Figure 2H). The intracellular utrophin staining was observed in both regenerating (MHCd-positive) and non-regenerating fibers (Supplemental Figures 2G, H). Thus, utrophin is upregulated in muscle fibers from the patient with the ex10-60 deletion but is not localized as well to the sarcolemma in all myofibers, which contrasts with sarcolemmal-based utrophin upregulation observed in typical DMD patients.

Based on these results, we propose the following model explaining the unexpectedly early and severe phenotype in this patient with an in-frame *DMD* deletion of exons 10-60 (Figure 2C). The deletion results in an internally shortened ~112 kDa protein that localizes to the membrane, but lacks critical functional regions, such as the actin binding domain. Contrary to a typical DMD patient, absence of these functional domains is not partially rescued by utrophin upregulation, since utrophin is displaced from the membrane by the mutant internally deleted dystrophin, which is thereby exerting a dominant negative effect on utrophin localization. Thus, we propose that both functional domain deletion and the absence of partial functional rescue by utrophin underlie the unusually early and severe phenotypic presentation in our patient, more severe compared to the typical presentation of DMD.

Discussion

We report a DMD patient with a considerably more severe (similar to a congenital muscular dystrophy) phenotype compared to a typical DMD, despite having an in-frame deletion, a mutation type usually associated with a milder Becker muscular dystrophy. The deletion identified in our patient (exons 10-60) is to our knowledge the largest reported in-frame deletion in the dystrophin gene [1,2,10–13]. This deletion involves all spectrin-like repeats of the rod domain and is expected to remove actin binding sites important for interactions with cytoskeleton, while preserving the β-dystroglycan binding regions located in the CR domain (Figure 1E). Our findings suggest that the normal sarcolemmal localization of the mutated dystrophin competitively prevents utrophin from taking dystrophin's place to partially compensate for the dystrophin deficiency and thus acts additionally in a dominant negative fashion on utrophin localization. The molecular mechanism of our patient's phenotype may therefore be functionally similar to the molecular defect in the severely dystrophic *dko* mouse, where both utrophin and functional dystrophin are absent from the muscle membrane [14,15]. Utrophin expression at the sarcolemma is also absent in Dp116/mdx4cv mice that express a dystrophin product lacking N-terminus and are more severely affected than their mdx4cv littermates[16]. Finally, *mdx* mice expressing a micro-dystrophin construct lacking all 24 spectrin-like repeats of the rod domain showed no rescue and had a more severe muscle phenotype compared to *mdx* mice[17]. Our report is the first in-human observation to support the deleterious nature of such extensively internally deleted dystrophin constructs. It also suggests that with less utrophin membrane association Duchenne muscular dystrophy may present with symptoms overlapping those of a congenital muscular dystrophy.

Other pathological mechanisms induced by the large in-frame ex10-60 deletion in our patient could also potentially participate in the phenotypic presentation. For example, a

protein conformational change could affect the remaining interactions with other structural muscle proteins, further contributing to the functional deficiency of this internally deleted dystrophin. For instance, certain missense variants have been suggested to disrupt the interactions between dystrophin and beta-dystroglycan through this mechanism, inducing a severe phenotype, despite apparently normal membrane expression of these proteins [18,19]. Alternatively, since the internal dystrophin promoters Dp260, Dp140 and Dp116 (located before exon 30, exon 34 and exon 56 respectively) are deleted in our patient, their loss could also play a confounding role[20].

Our findings may have relevance to the development of therapeutic strategies in DMD. First, our observations support the concept that utrophin has a role in mitigating the phenotype of dystrophin deficiency, as absence of sarcolemmal utrophin in our patient is associated with an unusually early and severe phenotype. Second, our study suggests that there may be a lower size limit for the construction of mini- and micro-dystrophins for delivery in AAV to dystrophin-deficient muscle[21–23]. We show in an actual clinical scenario that if the basic functionality of a dystrophin construct is not preserved, introducing this construct into patient muscle cells could be deleterious.

Limitations of Study

The limitation of our study is the small sample size, since the deletion of the almost entire dystrophin rod domain is only present in our single case. Description of another case with a similar deletion having the same effect on utrophin mis-localization would strengthen our conclusions.

Acknowledgments

We thank the affected individual and his family for their participation in this study. We also thank Dr. Jeffrey Chamberlain (University of Washington School of Medicine, Seattle, WA) for helpful discussion. We thank Aria Attia for his involvement in this project. This work was supported by a grant from MDA USA (MDA3896) and by grant number R01AR051999 from NIAMS/NIH to C.G.B. The work in C.G. Bönnemann's laboratory is supported by intramural funds from the NIH National Institute of Neurological Disorders and Stroke.

Author Contributions section:

Writing and editing SG, JS, YZ, MY, CB; original draft – JS, YZ, MY, CB; data analysis – SG, JS, YZ, MY, SD, CB, All authors contributed to the conception of the work and interpretation of the data. SG, YZ, SD, CB had unrestricted access to all data. All authors agreed to submit the manuscript, read and approved the final draft. They take full responsibility of its content, including the accuracy of the data.

Declaration of interests: The authors declare no competing interests.

Inclusion and diversity: We support inclusive, diverse, and equitable conduct of research.

Main figure titles and legends

Figure 1. Large in frame intragenic deletion in the *DMD* gene causes a severe muscular dystrophy. **A**. Clinical examination of patient at age of 3 ½ years. A significant head lag is noted on traction. Hypotonia of the legs is also present in this frog-legged position. **B**. PCR on genomic DNA from patient and an unaffected control shows an intragenic deletion of exons 10 to 60 of the *DMD* gene. Primer pairs specific to exons 8 and exon 61 amplify bands in both control and patient samples. There is no amplification of exons 10 and 60 in the patient sample, while the corresponding bands are present in the control genomic DNA. **C**. Sanger sequencing results of the abnormal junction between the *DMD* exons 9 and 61 in the cDNA from the patient, showing that the deletion is in-frame. RT-PCR on the muscle mRNA from the patient was performed using primers in the exons 9 and 62. **D**. Western blot analysis shows that the intragenic *DMD* deletion removes the central rod, while the C-terminal domain is preserved. No dystrophin-specific bands are detected in the patient's muscle tissue on the western blot analysis using the antibody directed against the central rod domain (DYS1). Probing the same membrane with the C-terminal specific antibody revealed a strong band of ~100kDa, corresponding to the expected molecular weight of the internally deleted dystrophin product (star). No dystrophin-specific bands were detected in the muscle lysates from three DMD patients carrying a truncating pathogenic variant. The full-length dystrophin was detected in the unaffected control muscle sample with both antibodies (triangles). Loading control with anti-tubulin antibody is shown. **E.** Deletion of the exons 10 to 60 is predicted to remove almost the entire central rod domain (deleted amino acids: His321-Gln3028). The internally deleted dystrophin from the patient is predicted to have the end of the hinge 1 joined directly to the final 12 amino acids of the repeat 24. The ABD and NTBD domains position were taken from [24]. Hinge 1 aa253-327, hinge 4 aa3041-3112 [25]. Antibody epitopes: DYS3 aa321-494, DYS1 aa1181-1388, DYS2 aa3669-3685 (Leica Biosystems). ABD, actin binding domain; N, N-terminal; H, hinge; R, spectrin-like repeats; MTBD, microtubule binding domain; CR, cysteine-rich; CT, C-terminal

Figure 2. Utrophin is upregulated in the patient with the intragenic DMD deletion but fails to localize to the sarcolemmal membrane. **A**. Western blot on muscle lysates from an unaffected control, the patient with the intragenic *DMD* deletion and a DMD patient carrying a truncating pathogenic variant. Utrophin is upregulated in both DMD patients, but it is retained intracellularly in most muscle cells in the patient with del ex10-60. **B-D.** Immunohistochemical staining using the utrophin-specific antibody on the muscle biopsy sections from an unaffected control, the patient with the intragenic *DMD* deletion, and a DMD patient carrying a truncating pathogenic variant. **E**. In normal muscle cells, dystrophin stabilizes the dystrophin-associated glycoprotein complex (DAPC) at the sarcolemmal membrane and binds actin among other cytoskeletal components. DMD patients lack functional dystrophin leading to the DAPC destabilization. Lack of certain dystrophin functions are compensated by a related protein, utrophin, that also binds actin and the DAPC. Expression of utrophin is upregulated in a typical DMD patient, leading to a strong utrophin staining at the sarcolemmal membrane. In our patient, the in-frame DMD deletion results in a much shorter mutant dystrophin protein that is able to stabilize the dystrophin-associated glycoprotein complex, but is lacking critical functional regions, such as the actin binding domain. The utrophin expression is increased in this patient muscles, but the utrophin molecules are displaced from the sarcolemma by the mutant dystrophin and are retained intracellularly. Utrophin is not able to partially rescue the dystrophin absence, leading to the unusually early and severe phenotypic presentation in our patient.

STAR Methods text

RESOURCE AVAILABILITY

Lead contact

Further information and requests for resources and reagents should be directed to and will be fulfilled by the lead contact, Carsten G. Bönnemann, M.D (carsten.bonnemann@nih.gov).

Materials availability

This study did not generate new unique reagents.

Data and code availability

Data: all data reported in this paper will be shared by the lead contact upon request.
Code: this paper does not report original code.
Any additional information required to reanalyze the data reported in this paper is available from the lead contact upon request.

EXPERIMENTAL MODEL AND SUBJECT DETAILS

Human subject

The data reported in this study obtained from one male patient during the period from 6m to 9y7m. Informed consent from the patient's parents was obtained (IRB approval 2002-6-2846, The Children's Hospital of Philadelphia, PA, USA and NIH Protocol 12-N-0095 approved by the Institutional Review Board of the National Institute of Neurological Disorders and Stroke, National Institutes of Health (NIH)). Information on gender and socioeconomic status was not collected.

METHOD DETAILS

Genomic DNA and cDNA analysis of *DMD* locus

Total RNA was extracted from frozen homogenized muscle tissue from the patient and a normal control. cDNA was prepared from 1 µg of total RNA with SuperScript® III Reverse Transcriptase (Life Technologies). cDNA was amplified using a forward primer located in the exon 9 (5'- TGCCAAGGCCACCTAAAGTGACTA-3') and a reverse primer in the exon 62 (5'- CACTTTGTTTGGCGAGATGGCTCT-3') using Taq DNA polymerase (Life Technologies), followed by Sanger sequencing of the obtained fragments. The obtained sequences were compared to the sequence of human *DMD* transcript NM_004006.2. The deletion was confirmed by a series of four PCR amplifications of the exons 8, 10, 60 and 61 on the genomic DNA from the patient and from a normal control. The following primers were used: exon8F 5'- GGCCTCATTCTCATGTTCTAATTAG-3', exon8R 5'- GTCCTTTACACACTTTACCTGTTGAG-3', exon10F: 5'-GGAACAATCTGCAAAGAC-3', exon10R: 5'-AAAGGATGACTTGCCATTATAAC-3', exon60F 5'- AGGAGAAATTGCGCCTCTGAAAGAGAACG-3', exon60R 5'- CTGCAGAAGCTTCCATCTGGTGTTCAGG-3', exon61F: 5'-CATTGTTTTAATTGTTCCTCATT-3', exon61R: 5'- TTCAACTCTTAATTCTTTTGTTTTT -3'.

Immunoblotting

Frozen muscle tissues from the patient, a normal control, and two unrelated DMD patients were lysed, followed by electrophoresis on a 3-8% Tris-Acetate SDS-PAGE gel and transferred onto a polyvinylidene difluoride membrane. The membrane was first incubated overnight at 4°C with mouse anti-dystrophin rod domain antibody (NCL-DYS1, Leica Biosystems) and rabbit anti-dystrophin C-terminus antibody (ab15277, Abcam), followed with IRDye 800CW conjugated goat anti-mouse secondary antibody and IRDye 680RD conjugated goat anti-rabbit secondary antibody. After stripping, the membrane was re-blotted with rabbit anti-tubulin antibody (11224-1-AP, proteintech) followed with 680RD conjugated goat anti-rabbit secondary antibody. The immunoblotting signal detection was performed with Odyssey Clx system (Licor). For utrophin protein detection, the membrane was incubated with mouse anti-utrophin monoclonal antibody (MANCHO3 (8A4), Developmental Studies Hybridoma Bank, University of Iowa, Iowa City, Iowa) overnight at 4°C, washed and incubated with HRP-conjugated secondary antibody at room temperature for 1 hour. The signal was detected with ECL (Life Technologies).

Immunohistochemistry

9 µm frozen muscle tissue sections were incubated overnight at 4°C labeled with monoclonal antibodies directed against N-terminal part of dystrophin (NCL-DYS3, Leica Biosystems, recognizing aa321-494), central rod domain of dystrophin, (NCL-DYS1, Leica Biosystems, recognizing aa1181-1388), C-terminal domain of dystrophin (NCL-DYS2, Leica Biosystems, recognizing aa3669-3685), utrophin (NCL-DRP2, Leica Biosystems), developmental myosin heavy chain (NCL-MHCd, Leica Biosystems), beta-Dystroglycan (NCL-b-DG, Leica Biosystems), and gamma-Sarcoglycan (NCL-g-SARC, Leica Biosystems). After washing, the sections were incubated with a secondary antibody goat anti-mouse 488 followed by DAPI staining. Sections were analyzed using laser scanning confocal microscopy with a 40x objective.

Supplemental video.

Clinical examination of patient. Related to Figure 1.

Supplemental figure titles and legends

Supplemental Figure 1. Internally deleted dystrophin correctly localizes to sarcolemma and stabilizes the dystroglycan complex.

Immunohistochemical staining using the antibody specific to the N-terminal part of the rod domain (DYS3) on the muscle biopsy sections from the patient with the intragenic *DMD* deletion (**A**), an unaffected control (**B**) and a DMD patient carrying a truncating pathogenic variant (**C**). Immunohistochemical staining using the antibody specific to the central part of the rod domain (DYS1) on the muscle biopsy sections from the patient with the intragenic *DMD* deletion (**D**), an unaffected control (**E**) and a DMD patient carrying a truncating pathogenic variant (**F**). Biopsy sections from both patients showed no staining with these antibodies, while a strong sarcolemmal labelling was detected in the control section. Immunohistochemical staining using the antibody

specific to the C-terminal domain of dystrophin protein (DYS2) on the muscle biopsy sections from the patient with the intragenic *DMD* deletion (**G**), an unaffected control (**H**) and a DMD patient carrying a truncating pathogenic variant (**I**). Muscle biopsy sections from the patient with the ex10-60 *DMD* deletion and from a healthy control demonstrated strong labelling at the sarcolemma with the C-terminal antibody DYS2, while no staining was observed on the biopsy section from a DMD patient. Immunohistochemical staining using the antibody specific to the β-dystroglycan (β-DG) on the muscle biopsy sections from the patient with the intragenic *DMD* deletion (**J**), an unaffected control (**K**) and a DMD patient carrying a truncating pathogenic variant (**L**). Muscle tissue from patient with the intragenic *DMD* deletion showed relatively normal expression of β-dystroglycan, while the muscle biopsy from a patient with a truncating *DMD* variant showed nearly complete absence of β-dystroglycan staining comparing to the control biopsy. Scale bar 50μm.

Supplementary figure 2. Ex10-60 *DMD* deletion is associated with intracellular utrophin staining in both regenerating and non-regenerating fibers, while preserving membrane γ-sarcoglycan staining.

Immunohistochemical staining using the antibody specific to the γ-sarcoglycan (γ- SG) on the muscle biopsy sections from the patient with the intragenic *DMD* deletion (**A**), an unaffected control (**B**) and a DMD patient carrying a truncating pathogenic variant (**C**). Membrane expression of the γ-sarcoglycan was observed in both patients and the control sample. **D-F**. Utrophin staining is increased on the sarcolemmal membrane in muscle sections from DMD patients. Immunohistochemical staining using a utrophin-specific antibody on the muscle biopsy sections from three unrelated patients carrying truncating pathogenic variants in the *DMD* gene. Endothelial staining typically observed with anti-utrophin staining (Helliwell *et al*. 1992, PMID: 1483043) is marked with a circle "○". **G-H**. Intracellular utrophin staining is observed in both regenerating (MHCd-positive) and non-regenerating fibers. Serial sections from our patient's muscle biopsy were stained with anti-MHCd and anti-utrophin antibodies. Several regenerating fibers are marked with an asterisk "*" in the panel G. These fibers, as well as the adjacent MHCd-negative fibers, exhibit intracellular staining with the anti-utrophin antibody in the panel H. Scale bar 50μm.

References

1. Aartsma-Rus, A., Van Deutekom, J. C. T., Fokkema, I. F., Van Ommen, G.-J. B. & Den Dunnen, J. T. Entries in the Leiden Duchenne muscular dystrophy mutation database: an overview of mutation types and paradoxical cases that confirm the reading-frame rule. *Muscle Nerve* **34**, 135–144 (2006).
2. Beggs, A. H. *et al.* Exploring the molecular basis for variability among patients with Becker muscular dystrophy: dystrophin gene and protein studies. *Am J Hum Genet* **49**, 54–67 (1991).
3. Khurana, T. S. *et al.* Immunolocalization and developmental expression of dystrophin related protein in skeletal muscle. *Neuromuscul Disord* **1**, 185–194 (1991).
4. Mizuno, Y., Nonaka, I., Hirai, S. & Ozawa, E. Reciprocal expression of dystrophin and utrophin in muscles of Duchenne muscular dystrophy patients, female DMD-carriers and control subjects. *J Neurol Sci* **119**, 43–52 (1993).
5. Mizuno, Y., Yoshida, M., Nonaka, I., Hirai, S. & Ozawa, E. Expression of utrophin (dystrophin-related protein) and dystrophin-associated glycoproteins in muscles from patients with Duchenne muscular dystrophy. *Muscle Nerve* **17**, 206–216 (1994).
6. Bittner, R. E. *et al.* Sarcolemmal expression of dystrophin C-terminus but reduced expression of 6q-dystrophin-related protein in two DMD patients with large deletions of the dystrophin gene. *Neuromuscul Disord* **5**, 81–92 (1995).

7. Chevron, M. P., Echenne, B. & Demaille, J. Absence of dystrophin and utrophin in a boy with severe muscular dystrophy. *N Engl J Med* **331**, 1162–1163 (1994).
8. Janghra, N. *et al.* Correlation of Utrophin Levels with the Dystrophin Protein Complex and Muscle Fibre Regeneration in Duchenne and Becker Muscular Dystrophy Muscle Biopsies. *PLoS One* **11**, e0150818 (2016).
9. Kleopa, K. A., Drousiotou, A., Mavrikiou, E., Ormiston, A. & Kyriakides, T. Naturally occurring utrophin correlates with disease severity in Duchenne muscular dystrophy. *Hum Mol Genet* **15**, 1623–1628 (2006).
10. England, S. B. *et al.* Very mild muscular dystrophy associated with the deletion of 46% of dystrophin. *Nature* **343**, 180–182 (1990).
11. Fanin, M. *et al.* Duchenne phenotype with in-frame deletion removing major portion of dystrophin rod: threshold effect for deletion size? *Muscle Nerve* **19**, 1154–1160 (1996).
12. Mirabella, M. *et al.* Giant dystrophin deletion associated with congenital cataract and mild muscular dystrophy. *Neurology* **51**, 592–595 (1998).
13. Passos-Bueno, M. R., Vainzof, M., Marie, S. K. & Zatz, M. Half the dystrophin gene is apparently enough for a mild clinical course: confirmation of its potential use for gene therapy. *Hum Mol Genet* **3**, 919–922 (1994).
14. Deconinck, A. E. *et al.* Utrophin-dystrophin-deficient mice as a model for Duchenne muscular dystrophy. *Cell* **90**, 717–727 (1997).
15. Grady, R. M. *et al.* Skeletal and cardiac myopathies in mice lacking utrophin and dystrophin: a model for Duchenne muscular dystrophy. *Cell* **90**, 729–738 (1997).
16. Judge, L. M., Haraguchiln, M. & Chamberlain, J. S. Dissecting the signaling and mechanical functions of the dystrophin-glycoprotein complex. *J Cell Sci* **119**, 1537–1546 (2006).
17. Harper, S. Q. *et al.* Modular flexibility of dystrophin: implications for gene therapy of Duchenne muscular dystrophy. *Nat Med* **8**, 253–261 (2002).
18. Goldberg, L. R. *et al.* A dystrophin missense mutation showing persistence of dystrophin and dystrophin-associated proteins yet a severe phenotype. *Ann Neurol* **44**, 971–976 (1998).
19. Vulin, A. *et al.* The ZZ domain of dystrophin in DMD: making sense of missense mutations. *Hum Mutat* **35**, 257–264 (2014).
20. Duan, D., Goemans, N., Takeda, S., Mercuri, E. & Aartsma-Rus, A. Duchenne muscular dystrophy. *Nat Rev Dis Primers* **7**, 13 (2021).
21. Jarmin, S., Kymalainen, H., Popplewell, L. & Dickson, G. New developments in the use of gene therapy to treat Duchenne muscular dystrophy. *Expert Opin Biol Ther* **14**, 209–230 (2014).
22. Lostal, W., Kodippili, K., Yue, Y. & Duan, D. Full-length dystrophin reconstitution with adeno-associated viral vectors. *Hum Gene Ther* **25**, 552–562 (2014).
23. Wang, B., Li, J. & Xiao, X. Adeno-associated virus vector carrying human minidystrophin genes effectively ameliorates muscular dystrophy in mdx mouse model. *Proc Natl Acad Sci U S A* **97**, 13714–13719 (2000).
24. Belanto, J. J. *et al.* Microtubule binding distinguishes dystrophin from utrophin. *Proc Natl Acad Sci U S A* **111**, 5723–5728 (2014).
25. Koenig, M. & Kunkel, L. M. Detailed analysis of the repeat domain of dystrophin reveals four potential hinge segments that may confer flexibility. *J Biol Chem* **265**, 4560–4566 (1990).

Figure 1

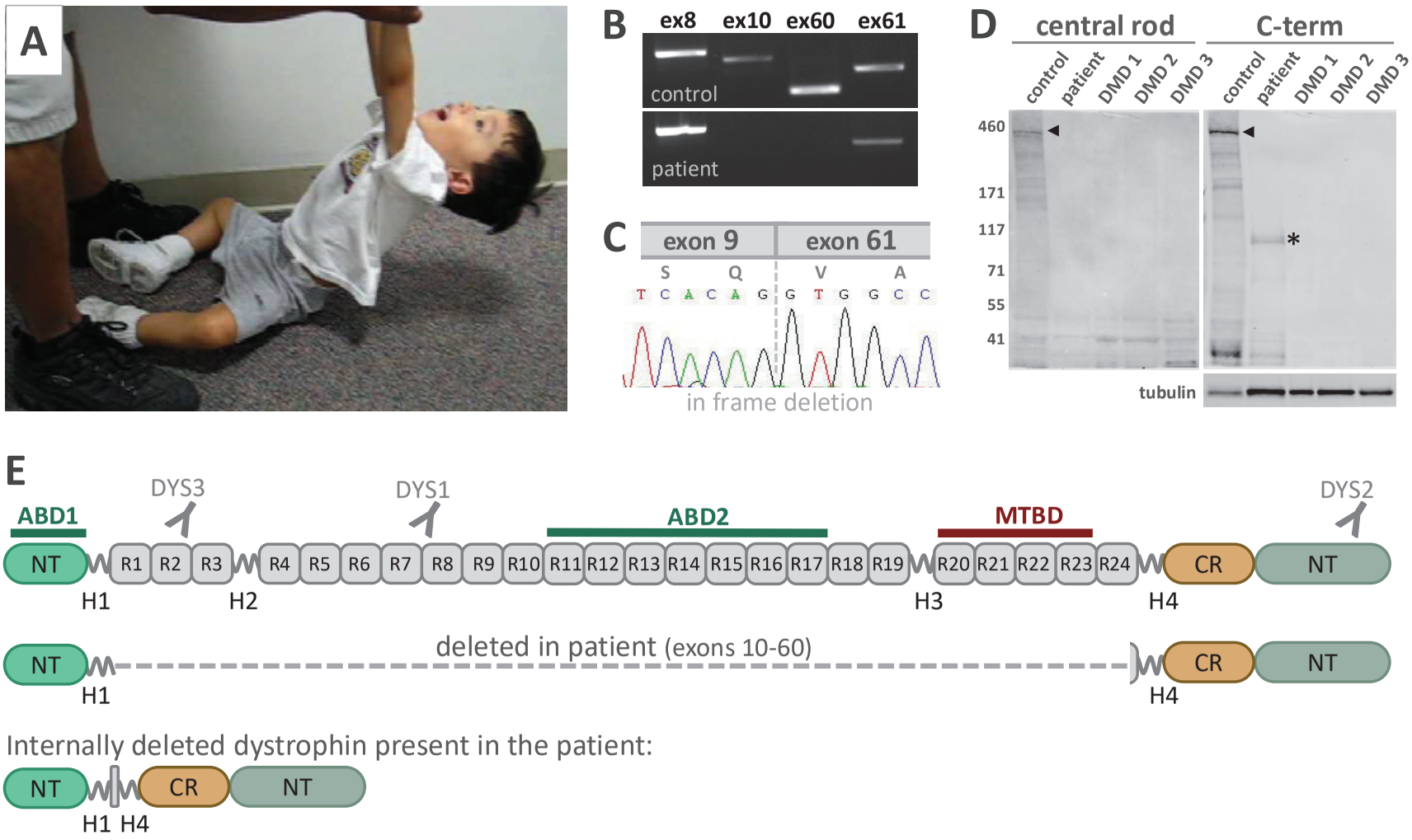
A
B
ex8
ex10
ex60
ex61
control
patient
C
exon 9
exon 61
S
Q
V
A
T C A C A G G T G G C C
in frame deletion
D
central rod
C-term
control
patient
DMD 1
DMD 2
DMD 3
460
171
117
71
55
41
tubulin
E
ABD1
DYS3
DYS1
ABD2
MTBD
DYS2
NT
R1 R2 R3 R4 R5 R6 R7 R8 R9 R10 R11 R12 R13 R14 R15 R16 R17 R18 R19 R20 R21 R22 R23 R24
CR
NT
H1
H2
H3
H4
deleted in patient (exons 10-60)
Internally deleted dystrophin present in the patient:

Figure 2

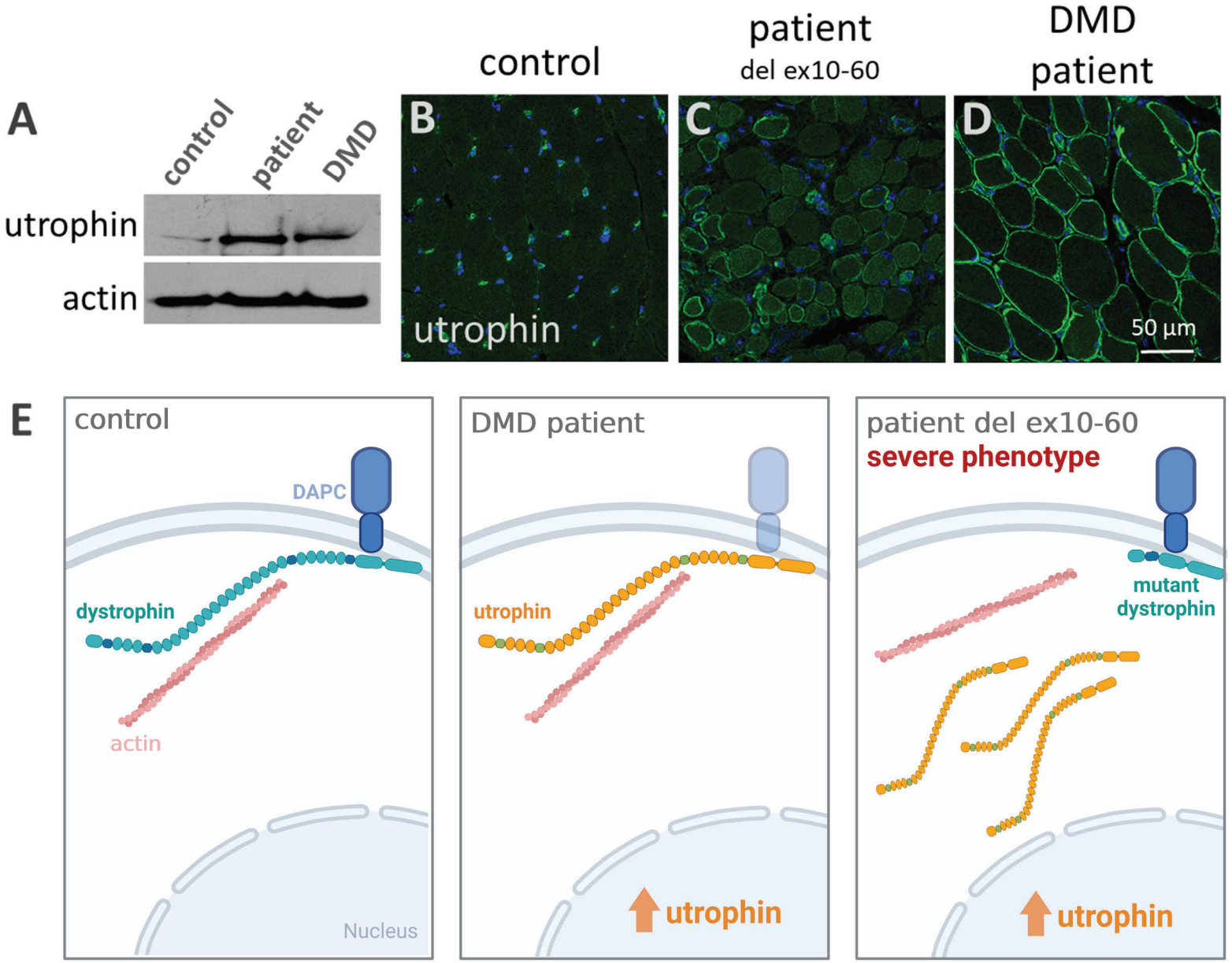
A
control
patient
DMD
utrophin
actin
control
patient
del ex10-60
DMD
patient
B
utrophin
C
D
50 µm
E
control
DAPC
dystrophin
actin
Nucleus
DMD patient
utrophin
utrophin
patient del ex10-60
severe phenotype
mutant
dystrophin
utrophin

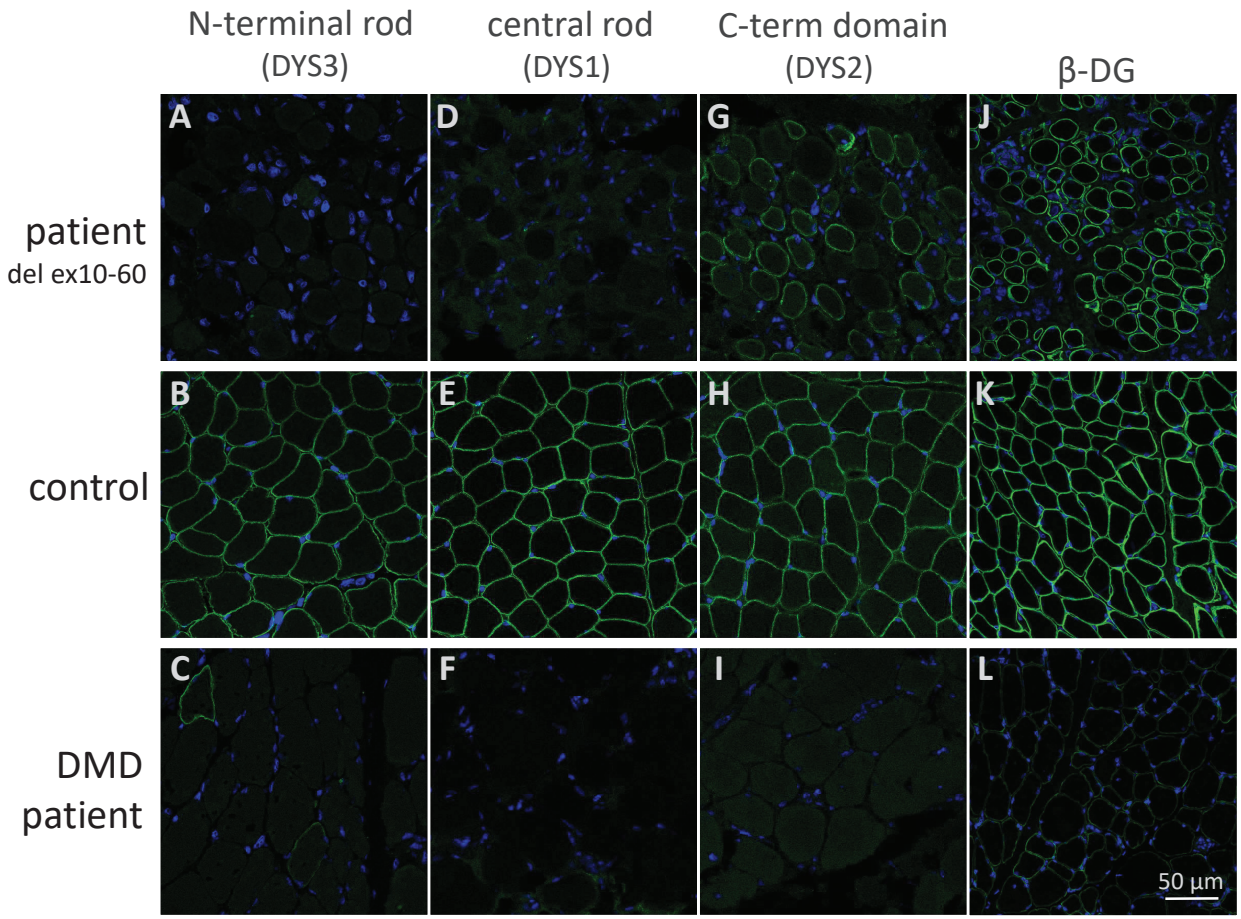

Supplemental Figure 1. Internally deleted dystrophin correctly localizes to sarcolemma and stabilizes the dystroglycan complex.

Immunohistochemical staining using the antibody specific to the N-terminal part of the rod domain (DYS3) on the muscle biopsy sections from the patient with the intragenic *DMD* deletion (**A**), an unaffected control (**B**) and a DMD patient carrying a truncating pathogenic variant (**C**). Immunohistochemical staining using the antibody specific to the central part of the rod domain (DYS1) on the muscle biopsy sections from the patient with the intragenic *DMD* deletion (**D**), an unaffected control (**E**) and a DMD patient carrying a truncating pathogenic variant (**F**). Biopsy sections from both patients showed no staining with these antibodies, while a strong sarcolemmal labelling was detected in the control section. Immunohistochemical staining using the antibody specific to the C-terminal domain of dystrophin protein (DYS2) on the muscle biopsy sections from the patient with the intragenic *DMD* deletion (**G**), an unaffected control (**H**) and a DMD patient carrying a truncating pathogenic variant (**I**). Muscle biopsy sections from the patient with the ex10-60 *DMD* deletion and from a healthy control demonstrated strong labelling at the sarcolemma with the C-terminal antibody DYS2, while no staining was observed on the biopsy section from a DMD patient. Immunohistochemical staining using the antibody specific to the β-dystroglycan (β-DG) on the muscle biopsy sections from the patient with the intragenic *DMD* deletion (**J**), an unaffected control (**K**) and a DMD patient carrying a truncating pathogenic variant (**L**). Muscle tissue from patient with the intragenic *DMD* deletion showed relatively normal expression of β-dystroglycan, while the muscle biopsy from a patient with a truncating *DMD* variant showed nearly complete absence of β-dystroglycan staining comparing to the control biopsy. Scale bar 50µm.

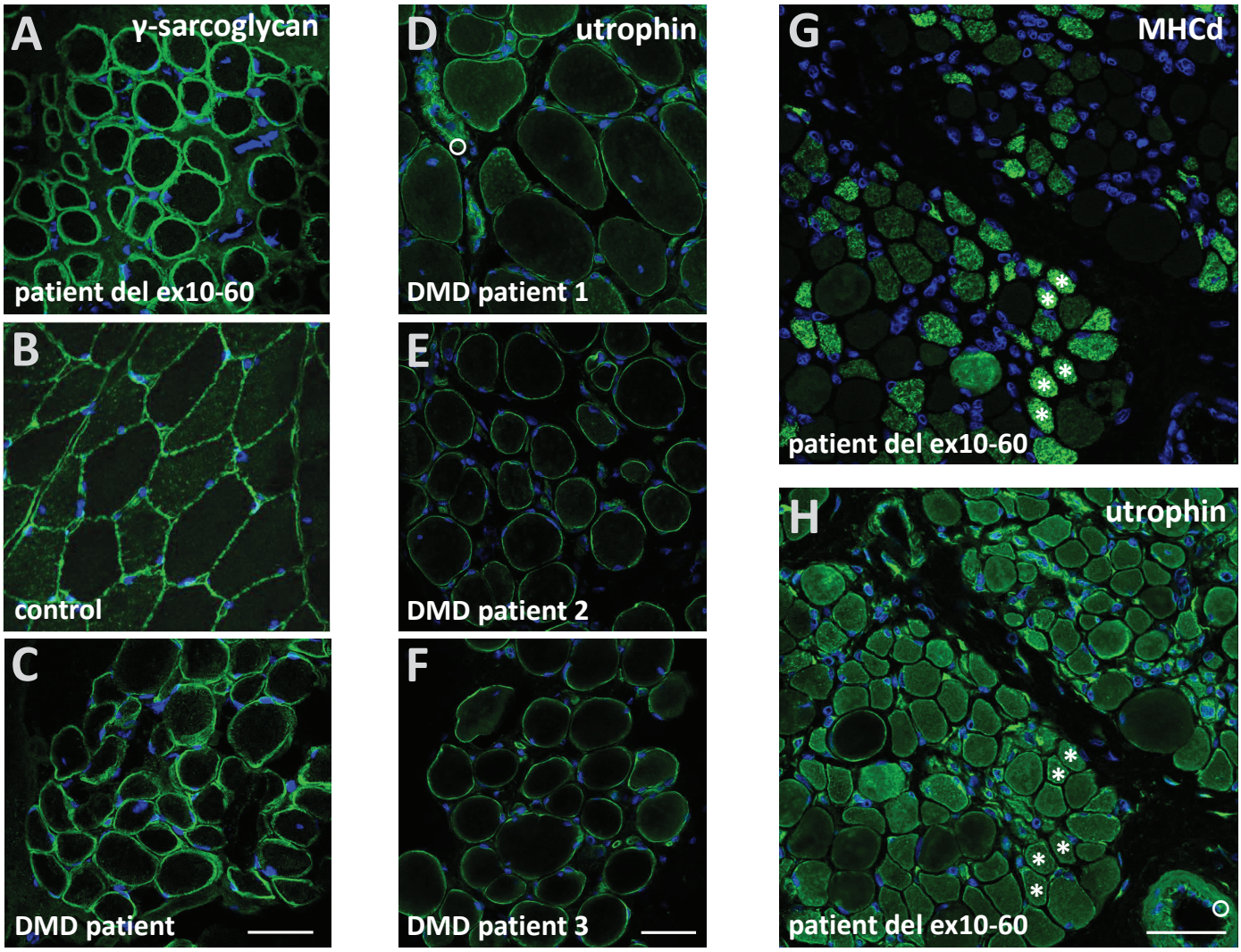

Supplementary figure 2. Ex10-60 *DMD* deletion is associated with intracellular utrophin staining in both regenerating and non-regenerating fibers, while preserving membrane γ-sarcoglycan staining.
Immunohistochemical staining using the antibody specific to the γ-sarcoglycan (γ- SG) on the muscle biopsy sections from the patient with the intragenic *DMD* deletion (**A**), an unaffected control (**B**) and a DMD patient carrying a truncating pathogenic variant (**C**). Membrane expression of the γ-sarcoglycan was observed in both patients and the control sample. **D-F**. Utrophin staining is increased on the sarcolemmal membrane in muscle sections from DMD patients. Immunohistochemical staining using a utrophin-specific antibody on the muscle biopsy sections from three unrelated patients carrying truncating pathogenic variants in the *DMD* gene. Endothelial staining typically observed with anti-utrophin staining (Helliwell *et al.* 1992, PMID: 1483043) is marked with a circle "○". **G-H**. Intracellular utrophin staining is observed in both regenerating (MHCd-positive) and non-regenerating fibers. Serial sections from our patient's muscle biopsy were stained with anti-MHCd and anti-utrophin antibodies. Several regenerating fibers are marked with an asterisk "*" in the panel G. These fibers, as well as the adjacent MHCd-negative fibers, exhibit intracellular staining with the anti-utrophin antibody in the panel H. Scale bar 50μm.

Key resources table

REAGENT or RESOURCE	SOURCE	IDENTIFIER
Antibodies		
Mouse anti- N-terminal part of dystrophin	Leica Biosystems	NCL-DYS3
Mouse anti-dystrophin rod domain antibody	Leica Biosystems	NCL-DYS1
Mouse anti- C-terminal domain of dystrophin	Leica Biosystems	NCL-DYS2
Rabbit anti-dystrophin C-terminus antibody	Abcam	ab15277
Rabbit anti-tubulin antibody	Proteintech	11224-1-AP
Mouse anti-utrophin antibody	Developmental Studies Hybridoma Bank, University of Iowa, Iowa City, Iowa	MANCHO3 (8A4)
Mouse anti-utrophin antibody	Leica Biosystems	NCL-DRP2
Mouse anti- developmental myosin heavy chain antibody	Leica Biosystems	NCL-MHCd
Mouse anti- beta-Dystroglycan antibody	Leica Biosystems	NCL-b-DG
Mouse anti- gamma-Sarcoglycan antibody	Leica Biosystems	NCL-g-SARC
Bacterial and virus strains		
N/A		
Biological samples		
Patient-derived muscle biopsy lysate	N/A	N/A
Patient-derived muscle biopsy frozen sections	N/A	N/A
Chemicals, peptides, and recombinant proteins		
N/A		
Critical commercial assays		
N/A		
Deposited data		
N/A		
Experimental models: Cell lines		
N/A		
Experimental models: Organisms/strains		
one male patient followed during the period 6m to 9y7m		
Oligonucleotides		
Forward exon 9 primer 5’- TGCCAAGGCCACCTAAAGTGACTA-3’		
Reverse exon 62 primer 5’-CACTTTGTTTGGCGAGATGGCTCT-3’		
Forward exon 8 primer 5’- GGCCTCATTCTCATGTTCTAATTAG-3’		

Reverse exon 8 primer 5’- GTCCTTTACACACTTTACCTGTTGAG-3’		
Forward exon 10 primer 5’-GGAACAATCTGCAAAGAC-3’		
Reverse exon 10 primer 5’-AAAGGATGACTTGCCATTATAAC-3’		
Forward exon 60 primer 5’- AGGAGAAATTGCGCCTCTGAAAGAGAACG-3’		
Reverse exon 60 primer 5’- CTGCAGAAGCTTCCATCTGGTGTTCAGG-3’		
Forward exon 61 primer 5’-CATTGTTTTAATTGTTCCTCATT-3’		
Reverse exon 61 primer 5’- TTCAACTCTTAATTCTTTTGTTTTT -3’		
Recombinant DNA		
N/A		
Software and algorithms		
N/A		
Other		

LIFE SCIENCE TABLE WITH EXAMPLES FOR AUTHOR REFERENCE

REAGENT or RESOURCE	SOURCE	IDENTIFIER
Antibodies		
Rabbit monoclonal anti-Snail	Cell Signaling Technology	Cat#3879S; RRID: AB_2255011
Mouse monoclonal anti-Tubulin (clone DM1A)	Sigma-Aldrich	Cat#T9026; RRID: AB_477593
Rabbit polyclonal anti-BMAL1	This paper	N/A
Bacterial and virus strains		
pAAV-hSyn-DIO-hM3D(Gq)-mCherry	Krashes et al.[1]	Addgene AAV5; 44361-AAV5
AAV5-EF1a-DIO-hChR2(H134R)-EYFP	Hope Center Viral Vectors Core	N/A
Cowpox virus Brighton Red	BEI Resources	NR-88
Zika-SMGC-1, GENBANK: KX266255	Isolated from patient (Wang et al.[2])	N/A
Staphylococcus aureus	ATCC	ATCC 29213
Streptococcus pyogenes: M1 serotype strain: strain SF370; M1 GAS	ATCC	ATCC 700294
Biological samples		
Healthy adult BA9 brain tissue	University of Maryland Brain & Tissue Bank; http://medschool.umaryland.edu/btbank/	Cat#UMB1455
Human hippocampal brain blocks	New York Brain Bank	http://nybb.hs.columbia.edu/
Patient-derived xenografts (PDX)	Children's Oncology Group Cell Culture and Xenograft Repository	http://cogcell.org/
Chemicals, peptides, and recombinant proteins		
MK-2206 AKT inhibitor	Selleck Chemicals	S1078; CAS: 1032350-13-2
SB-505124	Sigma-Aldrich	S4696; CAS: 694433-59-5 (free base)
Picrotoxin	Sigma-Aldrich	P1675; CAS: 124-87-8
Human TGF-β	R&D	240-B; GenPept: P01137
Activated S6K1	Millipore	Cat#14-486
GST-BMAL1	Novus	Cat#H00000406-P01
Critical commercial assays		
EasyTag EXPRESS 35S Protein Labeling Kit	PerkinElmer	NEG772014MC
CaspaseGlo 3/7	Promega	G8090
TruSeq ChIP Sample Prep Kit	Illumina	IP-202-1012
Deposited data		
Raw and analyzed data	This paper	GEO: GSE63473
B-RAF RBD (apo) structure	This paper	PDB: 5J17

Human reference genome NCBI build 37, GRCh37	Genome Reference Consortium	http://www.ncbi.nlm.nih.gov/projects/genome/assembly/grc/human/
Nanog STILT inference	This paper; Mendeley Data	http://dx.doi.org/10.17632/wx6s4mj7s8.2
Affinity-based mass spectrometry performed with 57 genes	This paper; Mendeley Data	Table S8; http://dx.doi.org/10.17632/5hvpvspw82.1
Experimental models: Cell lines		
Hamster: CHO cells	ATCC	CRL-11268
D. melanogaster: Cell line S2: S2-DRSC	Laboratory of Norbert Perrimon	FlyBase: FBtc0000181
Human: Passage 40 H9 ES cells	MSKCC stem cell core facility	N/A
Human: HUES 8 hESC line (NIH approval number NIHhESC-09-0021)	HSCI iPS Core	hES Cell Line: HUES-8
Experimental models: Organisms/strains		
C. elegans: Strain BC4011: srl-1(s2500) II; dpy-18(e364) III; unc-46(e177)rol-3(s1040) V.	Caenorhabditis Genetics Center	WB Strain: BC4011; WormBase: WBVar00241916
D. melanogaster: RNAi of Sxl: y[1] sc[*] v[1]; P{TRiP.HMS00609}attP2	Bloomington Drosophila Stock Center	BDSC:34393; FlyBase: FBtp0064874
S. cerevisiae: Strain background: W303	ATCC	ATTC: 208353
Mouse: R6/2: B6CBA-Tg(HDexon1)62Gpb/3J	The Jackson Laboratory	JAX: 006494
Mouse: OXTRfl/fl: B6.129(SJL)-Oxtr$^{tm1.1Wsy}$/J	The Jackson Laboratory	RRID: IMSR_JAX:008471
Zebrafish: Tg(Shha:GFP)t10: t10Tg	Neumann and Nuesslein-Volhard[3]	ZFIN: ZDB-GENO-060207-1
Arabidopsis: 35S::PIF4-YFP, BZR1-CFP	Wang et al.[4]	N/A
Arabidopsis: JYB1021.2: pS24(AT5G58010)::cS24:GFP(-G):NOS #1	NASC	NASC ID: N70450
Oligonucleotides		
siRNA targeting sequence: PIP5K I alpha #1: ACACAGUACUCAGUUGAUA	This paper	N/A
Primers for XX, see Table SX	This paper	N/A
Primer: GFP/YFP/CFP Forward: GCACGACTTCTTCAAGTCCGCCATGCC	This paper	N/A
Morpholino: MO-pax2a GGTCTGCTTTGCAGTGAATATCCAT	Gene Tools	ZFIN: ZDB-MRPHLNO-061106-5
ACTB (hs01060665_g1)	Life Technologies	Cat#4331182
RNA sequence: hnRNPA1_ligand: UAGGGACUUAGGGUUCUCUCUAGGGACUUAGGGUUCUCUCUAGGGA	This paper	N/A
Recombinant DNA		
pLVX-Tight-Puro (TetOn)	Clonetech	Cat#632162
Plasmid: GFP-Nito	This paper	N/A

cDNA GH111110	Drosophila Genomics Resource Center	DGRC:5666; FlyBase:FBcl0130415
AAV2/1-hsyn-GCaMP6- WPRE	Chen et al.[5]	N/A
Mouse raptor: pLKO mouse shRNA 1 raptor	Thoreen et al.[6]	Addgene Plasmid #21339
Software and algorithms		
ImageJ	Schneider et al.[7]	https://imagej.nih.gov/ij/
Bowtie2	Langmead and Salzberg[8]	http://bowtie-bio.sourceforge.net/bowtie2/index.shtml
Samtools	Li et al.[9]	http://samtools.sourceforge.net/
Weighted Maximal Information Component Analysis v0.9	Rau et al.[10]	https://github.com/ChristophRau/wMICA
ICS algorithm	This paper; Mendeley Data	http://dx.doi.org/10.17632/5hvpvspw82.1
Other		
Sequence data, analyses, and resources related to the ultra-deep sequencing of the AML31 tumor, relapse, and matched normal	This paper	http://aml31.genome.wustl.edu
Resource website for the AML31 publication	This paper	https://github.com/chrisamiller/aml31SuppSite

PHYSICAL SCIENCE TABLE WITH EXAMPLES FOR AUTHOR REFERENCE

REAGENT or RESOURCE	SOURCE	IDENTIFIER
Chemicals, peptides, and recombinant proteins		
QD605 streptavidin conjugated quantum dot	Thermo Fisher Scientific	Cat#Q10101MP
Platinum black	Sigma-Aldrich	Cat#205915
Sodium formate BioUltra, ≥99.0% (NT)	Sigma-Aldrich	Cat#71359
Chloramphenicol	Sigma-Aldrich	Cat#C0378
Carbon dioxide (^{13}C, 99%) (<2% ^{18}O)	Cambridge Isotope Laboratories	CLM-185-5
Poly(vinylidene fluoride-co-hexafluoropropylene)	Sigma-Aldrich	427179
PTFE Hydrophilic Membrane Filters, 0.22 μm, 90 mm	Scientificfilters.com/Tisch Scientific	SF13842
Critical commercial assays		
Folic Acid (FA) ELISA kit	Alpha Diagnostic International	Cat# 0365-0B9
TMT10plex Isobaric Label Reagent Set	Thermo Fisher	A37725
Surface Plasmon Resonance CM5 kit	GE Healthcare	Cat#29104988
NanoBRET Target Engagement K-5 kit	Promega	Cat#N2500
Deposited data		
B-RAF RBD (apo) structure	This paper	PDB: 5J17
Structure of compound 5	This paper; Cambridge Crystallographic Data Center	CCDC: 2016466
Code for constraints-based modeling and analysis of autotrophic *E. coli*	This paper	https://gitlab.com/elad.noor/sloppy/tree/master/rubisco
Software and algorithms		
Gaussian09	Frish et al.[1]	https://gaussian.com
Python version 2.7	Python Software Foundation	https://www.python.org
ChemDraw Professional 18.0	PerkinElmer	https://www.perkinelmer.com/category/chemdraw
Weighted Maximal Information Component Analysis v0.9	Rau et al.[2]	https://github.com/ChristophRau/wMICA
Other		
DASGIP MX4/4 Gas Mixing Module for 4 Vessels with a Mass Flow Controller	Eppendorf	Cat#76DGMX44
Agilent 1200 series HPLC	Agilent Technologies	https://www.agilent.com/en/products/liquid-chromatography
PHI Quantera II XPS	ULVAC-PHI, Inc.	https://www.ulvac-phi.com/en/products/xps/phi-quantera-ii/